Chapter 14

A protocol for single molecule translation imaging in xenopus retinal ganglion cells

Florian Ströhl[1,2,*], Julie Qiaojin Lin[2,3,4,*], Francesca W van Tartwijk[2], Hovy Ho-Wai Wong[3,5], Christine E Holt[3] and Clemens F Kaminski[2,4]

[1] Department of Physics and Technology, UiT The Arctic University of Norway, NO-9037 Tromsø, Norway
[2] Department of Chemical Engineering and Biotechnology, University of Cambridge, CB3 0AS, Cambridge, UK
[3] Department of Physiology, Development and Neuroscience, University of Cambridge, Downing Street, CB2 3DY, Cambridge, UK
[4] UK Dementia Research Institute at University of Cambridge, Department of Clinical Neurosciences, Island Research Building, Cambridge Biomedical Campus, CB2 0SL, Cambridge, UK
[5] Centre of Research in Neuroscience, Brain Repair and Integrative Neuroscience Programme, Department of Neurology and Neurosurgery, The Research Institute of the McGill University Health Centre, Montreal General Hospital, Montréal, QC H3A 1A4, Canada
* These authors contributed equally.

Abstract

Single molecule translation imaging (SMTI) is a straightforward technique for the direct quantification of local protein synthesis. The protein of interest is fused to a fast-folding and fast-bleaching fluorescent protein, allowing one to monitor the appearance of individual fluorescence events after photobleaching of extant proteins in the cell under investigation. The translation of individual molecules is then indicated by photon bursts of sub-second length that appear over a dark background. The method thus shares attributes with FRAP (fluorescence recovery after photobleaching) microscopy. Resulting datasets are similar to those generated by localization-based super-resolution microscopy techniques and can be used both to generate density maps of local protein production and to quantify the kinetics of local synthesis. The detailed protocol described in this chapter uses a Venus-β-actin fusion construct to visualize and measure the *β-actin* mRNA translational activity in *Xenopus* retinal ganglion cell growth cones upon Netrin-1 stimulation, which can be readily adapted for detecting translation events of other mRNAs in various cell types.

Key words Local protein translation, Localization microscopy, β-actin, Venus, Axonal navigation, Guidance cues, Netrin-1, Retinal ganglion cells

1 Introduction

1.1 Motivation

Translation is the process in which ribosomes synthesize specific polypeptide chains according to a DNA-encoded sequence blueprint, the messenger RNA (mRNA). Folding of the nascent polypeptide is necessary for it to function as an active protein. In neurons, ribosomes are found in the cell body, but they are also present in more distal compartments like dendrites and axons, where they synthesize proteins locally [1, 2].

Local translation can impart a certain regulatory autonomy to subcellular compartments, which is of great importance for axonal guidance during neurodevelopment. The tip of a growing axon (the growth cone) often navigates to a remote target region, for instance from the retina

to the optic tectum/superior colliculus in the brain, which requires it to respond to extracellular guidance cues by turning, advancing, or pausing in a timely manner [3–5]. Given the complexity of this task and the significant travel distance relative to the cell body length, growth cones must possess a high degree of autonomy to react sufficiently rapidly to spatially restricted cues [6]. Previous studies have provided evidence that local protein synthesis contributes to this fast and local response [7–12]. For instance, mRNA of the structural protein β-actin has long been known to be present in growth cones [13]. Local translation of *β-actin* mRNA occurs within ten minutes upon the application of a gradient of the extrinsic cue Netrin-1, causing the protein to accumulate on the gradient's near-side, as demonstrated by immunocytochemistry and using a translation reporter [8, 12].

The localized regulation of cue-mediated local translation represents a response mechanism distinct from the cell-wide shifts in gene expression, which are mediated by signaling pathways regulating transcription factor activity. Therefore, investigating the precise spatiotemporal dynamics of local translation activity at the single molecule level could provide valuable new insights. For example, it is not known precisely where in the growth cone new proteins are synthesized, how fast synthesis occurs in response to a cue, and whether it occurs repetitively in the same spot or singly in diverse sites (indicative of translation patterns of polysomes (complexes of single mRNA molecules and multiple ribosomes) or monosomes, respectively). To obtain intracytosolic localization data for the *de novo* synthesis of a protein of interest, fluorescence microscopy approaches are most suitable, as photo-depletion of pre-existing fluorescence allows event registration with minimal background within the native environment.

1.2 Imaging translation events

Two approaches to visualize translation have been developed recently, termed single molecule translation imaging (SMTI) and the nascent polypeptide fluorescent tagging method. The latter uses fluorescence amplification systems via multi-epitope tagging of tandem repeats of a peptide-binding site linked to the protein of interest by site-specific proteins fused to fluorescent proteins [14–16] or conjugated to dyes [17]. This chapter focuses on SMTI, which can provide a direct readout of translation [1, 2, 18].

An SMTI protocol involves several sample preparation and imaging steps. The fast-folding and fast-bleaching fluorescent protein Venus [19] is fused to a protein of interest, and the DNA encoding the fusion construct introduced into the specimen, for instance via chemical transfection or electroporation. The imaging protocol begins with illumination of the sample at high intensity for a short time period to reduce initial fluorescence and remove signal background caused by pre-existing protein. Subsequent imaging is performed at low illumination intensity. Each newly synthesized Venus protein is then detected as a short burst of fluorescence before becoming bleached, thus maintaining a background-free environment for high-precision readouts. A burst in fluorescence photons therefore signifies an individual translation event, which can be localized spatially via single molecule localization procedures and temporally within sequentially acquired imaging sequences (Figure 1b). Localizations of individual protein translation events are retrieved using specialized fitting software and appropriate filtering of detected events. Filtering can be performed using thresholds on the number of photons, the duration, shape, and size of candidate events. The information on locations and frames of occurrence of all detected events are then used to create translation rate density maps and translation rate graphs.

1.3 *Xenopus* as a model organism for SMTI

Xenopus laevis (African clawed frog) is a common model organism for the investigation of embryonic development and is suitable for imaging studies on neurodevelopment due to its relatively high tissue transparency. Retinal cultures produced from *Xenopus* are especially suitable for SMTI studies into axon guidance: the transparent retinal ganglion cell (RGC) axons are the only neuronal protrusions that exit the eye, they grow flatly onto the culture dish, and can be kept at room temperature. In this chapter, we detail a protocol for SMTI imaging of *β-actin* mRNA translation in RGC growth cones and the investigation of the effect of the guidance cue Netrin-1 on localised translation rates [1].

2 Methodology

2.1 Venus-β-actin plasmid construction

Construction of a plasmid encoding the fusion protein of interest with appropriate coding regions (CDSs) and untranslated regions (UTRs) can be achieved through amplification of separate DNA fragments and the subsequent insertion into a suitable plasmid.

Fragment A (*β-actin* 5'UTR and Venus) can be obtained by PCR amplification from the monomeric Venus plasmid (Addgene #27793) using a forward primer containing a BamHI site and *β-actin* 5'UTR sequence (underlined region in the forward primer) followed by 16 nucleotides complementary to the 5' end of Venus (start codon in bold), and a reverse primer adding a short linker sequence (AAGCTTGAATTCAAA) containing an EcoRI site.

Primers for Fragment A (*β-actin* 5'UTR and Venus):
Forward: 5'-TACTCGGATCCGGCTCAGTGACCCGCCCGCATAGAAAGGAGACAGTC TGTGTGCGTCCAACCCTCAGATCACA**ATG**GTTAGTAAGGGCG-3'
Reverse: 5'-GTATGAATTCAAGCTTTTTGTAAAGTTCATCC-3'

Subsequently, Fragment B (*β-actin* CDS and 3'UTR) can be obtained using the *Xenopus laevis* cDNA library as the template. Coding regions of interest for plasmid construction, namely the sequences of the *β-actin* mRNA CDS and 3'UTR, can be obtained from a suitable *Xenopus* cDNA library. The library can be constructed by extracting total mRNA from Stage 32 *Xenopus laevis* embryos using RNeasy Mini Kit (QIAGEN) and reverse transcribing using the SuperScript III First-Strand Synthesis System (Thermo Fisher Scientific) with the Oligo(dT) primer. The forward primer used in the PCR reaction contains the linker sequence with the EcoRI site and 16 nucleotides complementary to the 5' end of *β-actin* CDS, while the reverse primer includes 16 nucleotides complementary to the 3' end of *β-actin* 3'UTR and an XbaI site.

Primers for Fragment B (*β-actin* CDS and 3'UTR):
Forward: 5'-GCTTGAATTCAAAATGGAAGACGATATTG-3'
Reverse: 5'-CGTATCTAGAGTGAAACAACATAAGT-3'

The two fragments of the fusion construct can be inserted into a plasmid. As the backbone for plasmid construction, the pCS2+ vector (Addgene) was used, which contains a strong simian CMV promoter, followed by a multiple cloning site and an SV40 late polyadenylation site. Fragment A can be inserted into a linearized pCS2+ vector using BamHI and EcoRI restriction enzymes. Subsequently, fragment B can be inserted into the fragment A-containing pCS2+ plasmid using the EcoRI and XbaI restriction sites. The resulting Venus-β-actin construct consists of the following elements cloned into pCS2+ vector: 5'-(*β-actin* 5'UTR, Venus, a short linker (KLEFK), *β-actin* CDS and *β-actin* 3'UTR)-3' (Figure 1a).

2.2 *Xenopus laevis* embryos

Xenopus laevis eggs were fertilized *in vitro* and embryos were raised in 0.1x Modified Barth's Saline (MBS; 8.8 mM NaCl, 0.1 mM KCl, 0.24 mM $NaHCO_3$, 0.1 mM HEPES, 82 µM $MgSO_4$, 33 µM $Ca(NO_3)_2$, 41 µM $CaCl_2$) at 14-20°C and staged according to the tables of Nieuwkoop and Faber (Nieuwkoop and Faber, 1994). All animal experiments were approved by the University of Cambridge Ethical Review Committee in compliance with the University of Cambridge Animal Welfare Policy. This research has been regulated under the Animals (Scientific Procedures) Act 1986 Amendment Regulations 2012, following ethical review by the University of Cambridge Animal Welfare and Ethical Review Body (AWERB).

2.3 Targeted eye electroporation

Targeted eye electroporation can be performed as previously described [20, 21]. A "†" shape electroporation chamber suitable for stage 26-30 embryos can be modified from a Sylgard dish (Sigma) as described [20]. To anesthetize embryos during electroporation, 0.4 mg/ml tricaine methanesulfonate (MS-222) (Sigma) in 1x MBS, pH 7.5, is used. An anesthetized embryo is positioned along the longitudinal channel of the electroporation chamber, with its head positioned at the cross of the longitudinal and transverse channels. A pair of flat-ended platinum electrodes (Sigma) is held in place by a manual micromanipulator (World Precision Instruments) at the ends of the transverse channel. A glass capillary with a fine tip containing plasmid solution is inserted into the eye primordium of stage 26-30 embryos to inject 8x5-8 nl doses of 2 µg/µl Venus-β-actin plasmid driven by an air-pressured injector, such as a Picospritzer (Parker Hannifin). Immediately following the plasmid injection, 8 electric pulses of 50 ms duration at 1000 ms intervals are delivered at 18 V by a square wave generator, such as the TSS20 OVODYNE electroporator (Intracel). The embryos are recovered and raised in 0.1x MBS until they reach stage 32-35 as required for retinal cultures.

2.4 *Xenopus* retinal culture

For the retinal culture, dishes must be appropriately pre-treated to minimize background fluorescence. Glass bottom dishes (MatTek) are pre-treated with 5 M KOH (Sigma) for 1 hour, followed by 5-8 rinses with deionized water (Sigma), and are then left to dry in a hood (all culturing procedures should be performed in a laminar flow hood or a microbiological safety cabinet). They are next coated with 10 µg/ml poly-L-lysine (Sigma) and left overnight at room temperature. On the following day, excess poly-L-lysine is discarded from the dishes, which are then rinsed three times with double-distilled water and left in the hood until dry. Subsequently, the dishes are coated with 10 µg/ml laminin (Sigma) in L15 for 1-3 hours. Finally, the laminin solution is replaced with culture medium (60% (v/v) of L15 (GIBCO), 1% (v/v) Antibiotic–antimycotic (100x), in double-distilled water, pH 7.6-7.8, sterilized with 0.22µm pore-size filters), in which dissected eyes can be placed.

Embryos should be screened and washed before the retinal culture is commenced. Electroporated embryos at stage 32-35 should be screened for Venus fluorescence to check for successful electroporation. Successfully electroporated embryos are then rinsed three times in the embryo wash solution (0.1x MBS with 1% (v/v) Antibiotic–antimycotic (100x) (Thermo Fisher Scientific), pH 7.5, sterilized with 0.22µm pore-size filters) and anesthetized in MS-222 solution (0.04% (w/v) MS-222 and 1% (v/v) Antibiotic–antimycotic (100×) in 1x MBS, pH 7.5, filtered with 0.22µm filters). After transfer of the embryos to the Sylgard dish, the electroporated eye primordia are dissected out and washed three times in culture medium. A stereo microscope, 0.1-0.2 mm minutien pins (Fine Science Tools), pin holders (Fine Science Tools), forceps, and a Sylgard dish (Sigma) are needed for the eye dissection. Finally, the dissected eye primordia are placed in the center of the dish, and the cultures incubated at room temperature overnight. During this period, explanted eyes maintain their anatomical integrity in culture and only RGC axons exit the eye and grow on coverslips [22].

2.5 Optical setup

An SMTI optical setup consists of a standard widefield fluorescence microscope equipped with high-power lasers and a sensitive camera suitable for single molecule detection. Implementation is relatively straightforward if built around commercially available inverted microscope frames (e.g. Olympus IX73) [1]. For imaging of Venus, an illumination laser wavelength of 488 nm (Coherent Sapphire) can be used in combination with a 525/45 emission filter (Semrock) and a dichroic beam splitter (Chroma ZT405/488/561/640rpc). The laser beam must be circularly polarized by a quarter wave plate (AQWP05M-600, Thorlabs) to result in homogeneous excitation of fluorescent proteins (irrespective of their orientation). To collect data, an EMCCD camera (Andor iXon Ultra 897) is required with an effective optical pixel size near the optimum for single-molecule localization (ca. 120 nm) [23]. This can be achieved through use of a 100x magnification, 1.49 NA, oil immersion TIRF objective (Olympus UAPON100XOTIRF) in combination with an additional 1.3x magnification optical relay after the tube lens (e.g. via a TwinCam (CAIRN)) for a camera with physical pixel size of 16 µm (standard for EMCCD cameras).

The SMTI setup can be adapted to facilitate dual-colour imaging. For dual-colour imaging of mRFP as well as Venus, a 561 nm laser (Cobolt Jive) must be added in combination with a 600/37 emission filter (Semrock). This configuration allows easier identification and clearer visualization of transfected growth cones and is needed when brightfield identification is not feasible, e.g. when imaging in whole organisms [24]. Where simultaneous imaging is required, two identical EMCCD cameras (Andor iXon Ultra 897) can be used in conjunction with a TwinCam housing a dichroic beam splitter (Chroma T565spxr). The beam splitter must contain a 525/45 emission filter (Semrock) in the transmission direction to capture Venus fluorescence and a 600/37 emission filter (Semrock) in reflection to capture mRFP. Alterative fluorophore combinations are also possible, such as of Venus and Cy5. To capture Cy5 fluorescence, a 647 nm laser (MPB VFL-P-200-647) can be used in combination with a 680/42 emission filter (Semrock).

2.6 Imaging protocol

For SMTI, fluorescent axons emanating from the dissected eye are identified and traced to find their growth cones. An outgrowing fluorescent growth cone is selected and, prior to the bleaching step, imaged with low irradiance (<2 W cm^{-2}) in both fluorescence and bright field mode. These images can later be used to generate an outline image and to track growth cone health by comparison to an image taken once the SMTI acquisition sequence is completed. The growth cone is then photobleached for 10 s with an irradiance of 1.5 kW cm^{-2}. If pharmacological treatment or addition of a guidance cue is needed, they can be administered before or immediately after the photobleaching step. Afterwards, the flash-like recovery of Venus fluorescence is recorded with an exposure time of 200 ms at 5 Hz for 60 s to determine a baseline (non-stimulated) translation rate. Typically, a reduced intensity of around 0.3 kW cm^{-2} is used to ensure survival of the axons while simultaneously bleaching newly synthesized Venus. To study the effect of guidance cues, Netrin-1 (final concentration: 600 ng/ml, Sigma) or the same volume of culture medium as a control can then be added to the dish. As the dish is uncovered during drug application, the laser has to be switched off or appropriate laser safety goggles have to be used if the running acquisition should not be interrupted. After total SMTI acquisition period of 180 s, the second bright-field image is taken to check for growth cone health; retracted growth cones should be excluded from analysis. All imaging steps can be performed under epifluorescence as well as HILO (Highly Inclined and Laminated Optical sheet) or TIRF illumination. An EM gain of about 200 should be used on the EMCCD camera to ensure single molecule sensitivity. Furthermore, the field of illumination should be bigger than the size of the imaged field of view to bleach diffusing or transported fluorescent proteins from outside the growth cone prior to their entering the field of view.

2.7 Data processing and analysis software

Localizations of individual protein translation events are retrieved using maximum likelihood estimation with a Gaussian model fit, for example using the rapidSTORM software package [25]. RapidSTORM provides information on locations and frames of occurrence of all detected events, which can be used to create translation rate density maps and translation rate graphs in custom-written MATLAB scripts [1]. It is useful to filter out potentially non-translation events through appropriate thresholding; for instance, in most experimental conditions a threshold of ~500 photons per localization is appropriate to filter out noise and blinking events that do not stem from Venus.

To examine the spatial distribution of the translational events, a *Sholl* analysis [26] can be performed: each growth cone is divided into *n* evenly spaced concentric arcs. For n=5 arcs, a labelling of A1-A5 from central to peripheral domains can be used. Arc A5 is then set to circumscribe the outermost part of the growth cone (Figure 3d). Performing this analysis on control and treated samples visualizes and quantifies the translocation of translation sites, for example as they move from central domains to the periphery [20].

3 Notes

3.1 Plasmid construction

The advantage of fusing the Venus sequence to the 5'-end of the candidate gene CDS is that the mRNA sequence encoding Venus will be translated first, which shortens the time between the initiation of polypeptide synthesis and signal detection. Therefore, N-terminal Venus fusion is the preferable design, unless expression levels are found to be severely impaired for such constructs.

The untranslated regions of an mRNA are often crucial for its localization, stability and translation [27, 28]. If overexpression of the full-length protein impairs cellular physiology, a Venus sequence flanked by the 5' and 3' untranslated regions of the mRNA of interest can also be used in place of the fusion construct to investigate translational regulation.

3.2 Targeted eye electroporation

The expression level and ubiquity of Venus fluorescence can be influenced in several ways. The former should be carefully titrated, as high expression is associated with significant phototoxicity due to the prolonged photobleaching step and/or the increased reactive oxygen species resulting upon fluorophore excitation. Electroporation efficiency is known to decrease with increasing embryonic stage [20]. Therefore, eye-targeted electroporation is usually more efficient when performed at around stage 26 rather than in older embryos. In addition, choosing wider electrodes for electroporation can increase the number of fluorescence-positive cells.

3.3 *Xenopus* retinal culture

Screening and washing of the embryos can be carried out in parallel with incubation of the dishes with laminin solution.

3.4 Imaging protocol

An adaption of the SMTI protocol in the form of 'translation FRAP with low-power illumination' can also be used *in vivo* [24] and has, for instance, been employed for longer-term imaging of

the interplay between ribosome/RNA trafficking and the regulation of local protein synthesis during axon arborization. With this methodological variant, the challenges posed by the high intrinsic fluorescence background due to high power illumination and to some extent out-of-focus light in whole organisms can be overcome. Thus the docking of RNA granules at branching positions in conjunction with spatially and temporally resolved local translation could be correlated [24]. Recovery of fluorescence is in this case observed analogously to fluorescence recovery after photobleaching, FRAP, but used to indicate protein translation.

When highly mobile specimens like growth cones are imaged, it is useful to count all events in a small area even around and outside of the growth cone (e.g., a rectangular window that tightly crops the growth cones), to account for the high mobility of the growth cone filopodia.

3.5 Data processing, presentation, and analysis

The threshold used in the filtering step is found by manual selection of Venus flashes and determination of the *average* photon budget of a single emitting Venus molecule. The threshold value as well as the size of the emission PSF can be used as parameter settings in rapidSTORM [25]. Further optimization of the parameters can be performed on manually selected flashes in order to recognize as many real flashes as possible, while at the same time keeping the number of false positives as low as possible. For validation, the manual selection process can be repeated blindly by multiple independent researchers to minimize any bias occurring during the manual selection process [1]. The tracking option of rapidSTORM can be used to recombine photons emanating from the same fluorescent protein during a translation event over multiple frames to increase the number of photons per localization, but also to determine the *on-time* of the Venus flashes before bleaching. Another optimization parameter is the survival fraction as the high intensities required for SMTI can cause cell death due to phototoxicity. In this case, the employed illumination intensities can be reduced, but correspondingly longer durations are needed for the bleaching step.

Various examples for measurements of these parameters are displayed in Figure 2. A measured *on-time* of about 400 ms is displayed, which provides an indication of the average length of translation flashes. Changing of the intensity of the irradiation light can be used to tune this length to some degree, but care must be taken to avoid lethal dosages (compare panel (d)). The photon budget of a translation event can be calculated from the sum-value of pixel values belonging to single events, for instance by using a 5x5 pixel area around the brightest pixels. When the conversion factor of the camera is known, this value can be translated directly into the number of photons. As shown in panel (b), an average photon budget of around 500 photons was found in this example dataset, which indicates that each event is caused by the emission of single Venus molecules. As another control measure, the width of the PSF can be used to validate the diffraction-limited performance of the microscope (panel (c)).

4 Example results

Using the protocol described above, we studied the effect of Netrin-1 on *β-actin* mRNA translation rates and translocation of translation sites in navigating RGC growth cones.

Under no-treatment baseline conditions, single molecule translation events were detected at an average rate of ~10 events/min, which were located predominantly in the central domain of the growth cones (region A1 and A2 of the Sholl analysis depicted in Figure 3d). Translation in RGC growth cones was sporadic, with limited events reoccurring at the same location. This was in contrast to HEK293T cells, which exhibited hotspots of repetitive Venus-β-actin translation [1], or to hippocampal dendrites, in which the activity-regulated cytoskeletal-

associated (Arc) protein and the fragile X mental retardation protein (FMRP) undergo similar burst-like translation [18].

After translation was quantified for the baseline condition, the effect of the chemical guidance cue Netrin-1 was investigated. As displayed in the translation density maps in Figure 3a, the event rate was up to 0.5 events/s. The same dataset also provides even more detailed temporal information, in the form of a curve of instantaneous rate as function of time (Figure 3b). Remarkably, Netrin-1 stimulation led to a burst of *β-actin* translation starting 20 seconds post treatment and lasting for 30 seconds before gradually declining to lower, but still above baseline levels. The decline likely reflects a rapid desensitization of Netrin-1 receptors on the growth cone surface, which is known to occur within 1-2 minutes [29]. The initial increase in translation is clearly visible in a cumulative translation events plot, with the baseline translation of around 15 events/min and the event number doubled within the first minute after Netrin-1 application (Figure 3c). To examine the spatial distribution of the translational events, a Sholl analysis [26] was performed. The percentage of *β-actin* translation events located in the central arcs (A1 and A2) decreased upon Netrin-1 stimulation, whereas translational events located at the growth cone periphery (A3-A5) increased (Figure 3d). The Netrin-1-stimulated increase in fluorescence events was attenuated by pre-incubation of the samples with the translation inhibitor puromycin, indicating it was truly reflecting an increase in local *β-actin* translation rate. Incubation with puromycin also reduced the translation rate in HEK293T cells ($p=0.011$) but had no significant effect in growth cones not stimulated with Netrin-1, which could be a result of the already low baseline translation overshadowing the effect of puromycin ($p=0.57$).

5 Summary

SMTI is a technique that can be used to quantify the spatiotemporal dynamics of local translation, for instance to measure the effects of Netrin-1 on local *β-actin* mRNA translation in growth cones. Using SMTI, it has been shown that Netrin-1 transiently increases translation and that it causes relocation of potentially monosomal translation sites to the growth cone periphery. This result is in line with a previously described shift in translation activity inside of growth cones, which were exposed to an external gradient of guidance cues [8]. A rapid stimulating effect of Netrin-1 on *β-actin* local translation in RGC growth cones was observed in real-time and the concomitant shift of its translation towards the periphery of the growth cones measured. This translation localization pattern is consistent with the recently reported *β-actin* mRNA trafficking modes in axons and within growth cones [30, 31].

The SMTI protocol can be further developed to yield even richer insights. For example, the use of fluorescent proteins featuring shorter folding times and higher quantum yields will lead to improvements in temporal resolution and detection sensitivity. As the method has been shown to be capable of measurements of local translation rates at the single molecule level in axonal growth cones, it holds great potential for application to other model systems. The method is thus a powerful new tool for investigating signal-driven subcellular responses affecting protein synthesis.

6 References

1. Ströhl F, Lin JQ, Laine RF, et al (2017) Single Molecule Translation Imaging Visualizes the Dynamics of Local β-Actin Synthesis in Retinal Axons. Sci Rep 7:709. https://doi.org/10.1038/s41598-017-00695-7

2. Ifrim MF, Williams KR, Bassell GJ (2015) Single-Molecule Imaging of PSD-95 mRNA

Translation in Dendrites and Its Dysregulation in a Mouse Model of Fragile X Syndrome. J Neurosci 35:7116–7130. https://doi.org/10.1523/JNEUROSCI.2802-14.2015

3. Dickson BJ (2002) Molecular mechanisms of axon guidance. Science (80-) 298:1959–1964. https://doi.org/10.1126/science.1072165

4. O'Donnell M, Chance RK, Bashaw GJ (2009) Axon growth and guidance: receptor regulation and signal transduction. Annu Rev Neurosci 32:383–412. https://doi.org/10.1146/annurev.neuro.051508.135614

5. Kolodkin AL, Tessier-Lavigne M (2011) Mechanisms and molecules of neuronal wiring: A primer. Cold Spring Harb Perspect Biol 3:1–14. https://doi.org/10.1101/cshperspect.a001727

6. Harris WA, Holt CE, Bonhoeffer F (1987) Retinal axons with and without their somata, growing to and arborizing in the tectum of Xenopus embryos: a time-lapse video study of single fibres in vivo. Development 101:123–133

7. Campbell DS, Holt CE (2001) Chemotropic responses of retinal growth cones mediated by rapid local protein synthesis and degradation. Neuron 32:1013–1026. https://doi.org/10.1016/S0896-6273(01)00551-7

8. Leung K-M, van Horck FPG, Lin AC, et al (2006) Asymmetrical beta-actin mRNA translation in growth cones mediates attractive turning to netrin-1. Nat Neurosci 9:1247–56. https://doi.org/10.1038/nn1775

9. Piper M, Anderson R, Dwivedy A, et al (2006) Signaling mechanisms underlying Slit2-induced collapse of Xenopus retinal growth cones. Neuron 49:215–228. https://doi.org/10.1016/j.neuron.2005.12.008

10. Welshhans K, Bassell GJ (2011) Netrin-1-Induced Local beta-Actin Synthesis and Growth Cone Guidance Requires Zipcode Binding Protein 1. J Neurosci 31:9800–13. https://doi.org/10.1523/JNEUROSCI.0166-11.2011

11. Wu KY, Hengst U, Cox LJ, et al (2005) Local translation of RhoA regulates growth cone collapse. Nature 436:1020–4. https://doi.org/10.1038/nature03885

12. Yao J, Sasaki Y, Wen Z, et al (2006) An essential role for beta-actin mRNA localization and translation in Ca2+-dependent growth cone guidance. Nat Neurosci 9:1265–1273. https://doi.org/10.1038/nn1773

13. Bassell GJ, Zhang H, Byrd AL, et al (1998) Sorting of beta-actin mRNA and protein to neurites and growth cones in culture. J Neurosci 18:251–65

14. Wang C, Han B, Zhou R, Zhuang X (2016) Real-Time Imaging of Translation on Single mRNA Transcripts in Live Cells. Cell 165:990–1001. https://doi.org/10.1016/j.cell.2016.04.040

15. Yan X, Hoek TA, Vale RD, Tanenbaum ME (2016) Dynamics of Translation of Single mRNA Molecules In Vivo. Cell 165:976–989. https://doi.org/10.1016/j.cell.2016.04.034

16. Wu B, Eliscovich C, Yoon YJ, Singer RH (2016) Translation dynamics of single mRNAs in live cells and neurons. Science (80-) 352:1430–1435. https://doi.org/10.1126/science.aaf1084

17. Morisaki T, Lyon K, DeLuca KF, et al (2016) Real-time quantification of single RNA translation dynamics in living cells. Science (80-) 352:1425–1429. https://doi.org/10.1126/science.aaf0899

18. Tatavarty V, Ifrim MF, Levin M, et al (2012) Single-molecule imaging of translational

output from individual RNA granules in neurons. Mol Biol Cell 23:918–29. https://doi.org/10.1091/mbc.E11-07-0622

19. Nagai T, Ibata K, Park ES, et al (2002) A variant of yellow fluorescent protein with fast and efficient maturation for cell-biological applications. Nat Biotechnol 20:87–90. https://doi.org/10.1038/nbt0102-87

20. Falk J, Drinjakovic J, Leung KM, et al (2007) Electroporation of cDNA/Morpholinos to targeted areas of embryonic CNS in Xenopus. BMC Dev Biol 7:107. https://doi.org/10.1186/1471-213X-7-107

21. Wong HH-W, Holt CE (2018) Targeted electroporation in the CNS in Xenopus embryos. In: Xenopus protocols - methods for functional genomics and disease modeling, Methods in Molecular Biology

22. Cagnetta R, Frese CK, Shigeoka T, et al (2018) Rapid Cue-Specific Remodeling of the Nascent Axonal Proteome. Neuron 99:29-46.e4. https://doi.org/10.1016/j.neuron.2018.06.004

23. Thompson RE, Larson DR, Webb WW (2002) Precise nanometer localization analysis for individual fluorescent probes. Biophys J 82:2775–2783. https://doi.org/10.1016/S0006-3495(02)75618-X

24. Wong HH-W, Lin JQ, Ströhl F, et al (2017) RNA Docking and Local Translation Regulate Site-Specific Axon Remodeling In Vivo. Neuron 95:852-868.e8. https://doi.org/10.1016/j.neuron.2017.07.016

25. Wolter S, Löschberger A, Holm T, et al (2012) rapidSTORM : accurate , fast open-source software for localization microscopy. Nat Methods 9:1040–1. https://doi.org/10.1038/nmeth.2224

26. Sholl DA (1953) Dendritic organization in the neurons of the visual and motor cortices of the cat. J Anat 87:387–406

27. Xing L, Bassell GJ (2013) MRNA localization: An orchestration of assembly, traffic and synthesis. Traffic 14:2–14. https://doi.org/10.1111/tra.12004

28. Chabanon H, Mickleburgh I, Hesketh J (2004) Zipcodes and postage stamps: mRNA localisation signals and their trans-acting binding proteins. Brief Funct Genomic Proteomic 3:240–256. https://doi.org/10.1093/bfgp/3.3.240

29. Piper M, Salih S, Weinl C, et al (2005) Endocytosis-dependent desensitization and protein synthesis–dependent resensitization in retinal growth cone adaptation. Nat Neurosci 8:179–186. https://doi.org/10.1038/nn1380

30. Turner-Bridger B, Jakobs M, Muresan L, et al (2018) Single-molecule analysis of endogenous β-actin mRNA trafficking reveals a mechanism for compartmentalized mRNA localization in axons. Proc Natl Acad Sci 115:E9697–E9706. https://doi.org/10.1073/pnas.1806189115

31. Leung K-M, Lu B, Wong HH-W, et al (2018) Cue-Polarized Transport of β-actin mRNA Depends on 3′UTR and Microtubules in Live Growth Cones. Front Cell Neurosci 12:1–19. https://doi.org/10.3389/fncel.2018.00300

Figures

Figure 1

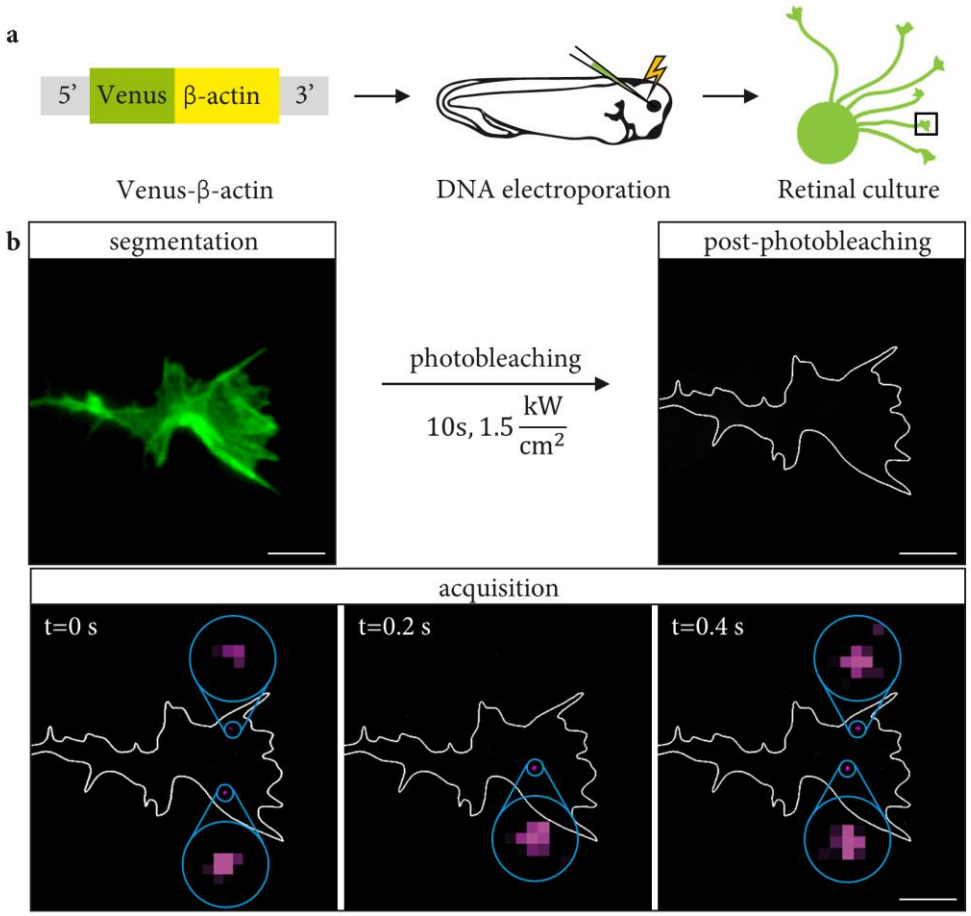

(a) A reporter construct, coding for e.g. Venus and β-actin, is electroporated into *Xenopus* eye primordia, which are dissected and cultured. (b) During imaging, a fluorescent image of a growth cone is acquired to segment the outline for later processing. Existing fluorescence is then photobleached using a brief pulse of laser irradiation. Subsequently, the translation of individual β-actin is recorded as individual Venus molecule emission. Scale bars are 5μm. Figure adapted from [1].

Figure 2

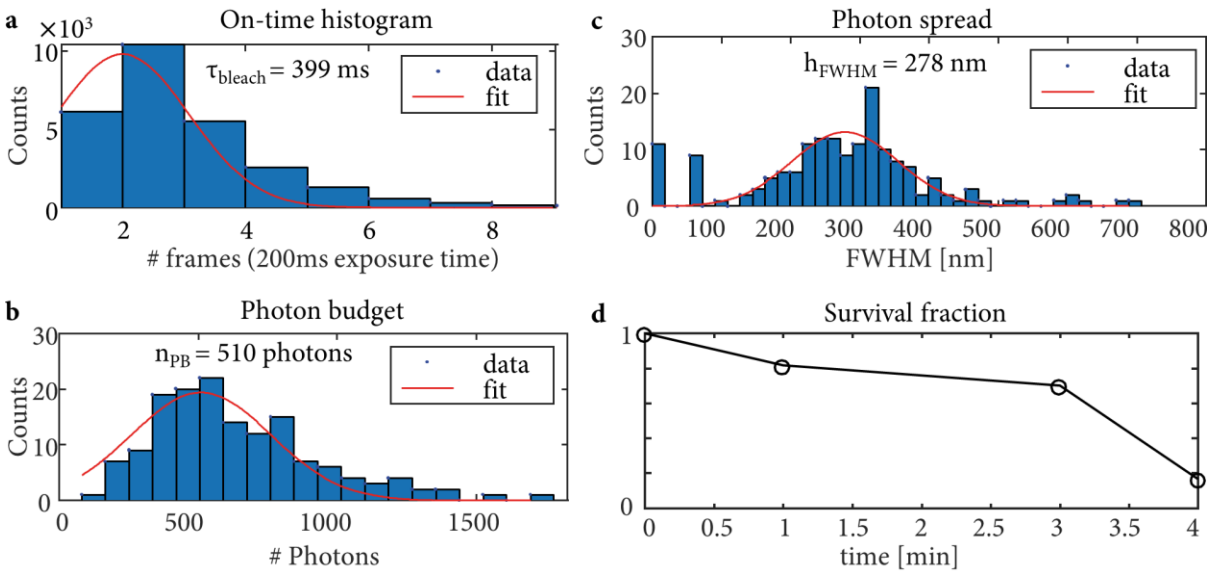

(a) The measured *on-time*, i.e. length of flashes, of the average Venus-β-actin molecule when using a laser irradiation of 0.3 kW/cm^2. (b) The average photon budget of a Venus-β-actin molecule as calculated from hundreds manually selected flashes, which were subjectively classified as stemming from Venus emission. (c) Width of the PSF. The broad distribution stems from flashes in different focal planes. (d) After 3 minutes of continuous imaging with 0.3 kW/cm^2 about 30% of axons started to retract, while 4 minutes of imaging caused most axons to be retracted. 46 axons were observed for this plot. Figure adapted from [1].

Figure 3

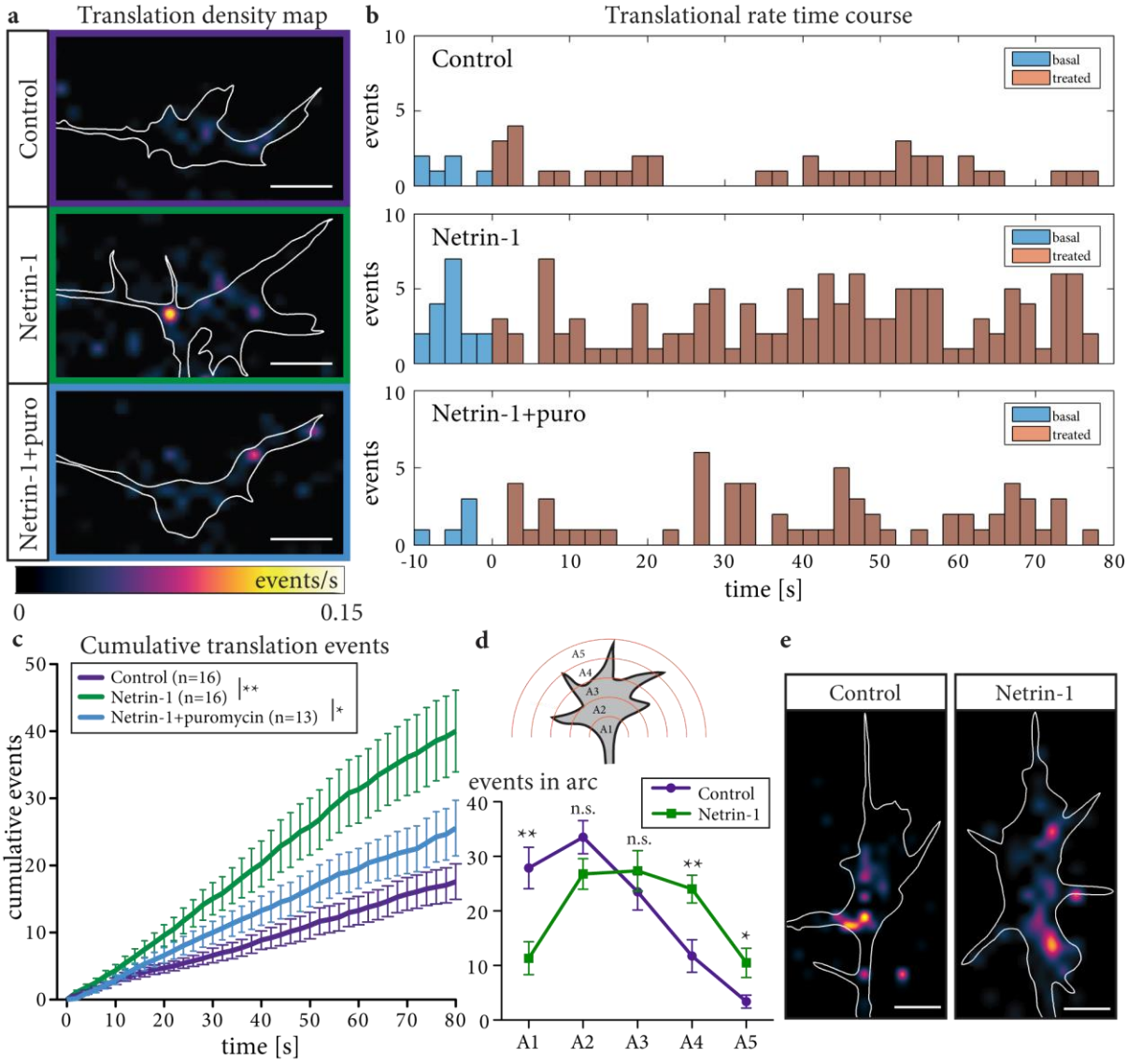

(a) Translation density maps for RGC growth cones in different conditions. (b) Respective translation rate time courses. The difference in the pre-treatment rates can be attributed to biological variability; the average pre-treatment rate between the two groups (n=16) was not significantly different (p=0.63). (c) Cumulative event rates per growth cone *p<0.05; **p<0.001; two-way ANOVA. (d) Sholl analysis on culture medium- or Netrin-1-treated growth cones shows the spatial distribution of translational events. The centre of 5 concentric circles is located at the base of the growth cone; the outermost circle is tangential to the growth cone tip. The radii are equidistant. Intracellular events within each arc in %. **p<0.001; Mann-Whitney Houston test; scale bars are 5µm. Error bars indicate standard error of the mean. In c, n is the number of growth cones. Figure adapted from [1].